

Supplemental materials for “Identification and differential production of ubiquinone-8 in the bacterial predator *Bdellovibrio bacteriovorus*”

Eileen M. Spain, Megan E. Núñez, Hyeong-Jin Kim, Ryan J. Taylor, Nicholas Thomas, Michael B. Wengen, Nathan F. Dalleska, Joseph P. Bromley, Kimberly H. Schermerhorn, and Megan A. Ferguson*

Table S1. Gradient flow conditions for semi-prep HPLC, used to purify the crude extract for compound analysis. Column flow rate was 4 mL min⁻¹ through an Agilent eclipse XDB 5 μ m column (9.4 x 250 mm).

Time (min)	Isopropyl alcohol : acetonitrile
0	30:70
20	30:70
26	40:60
29	70:30
33	70:30
33.5	30:70

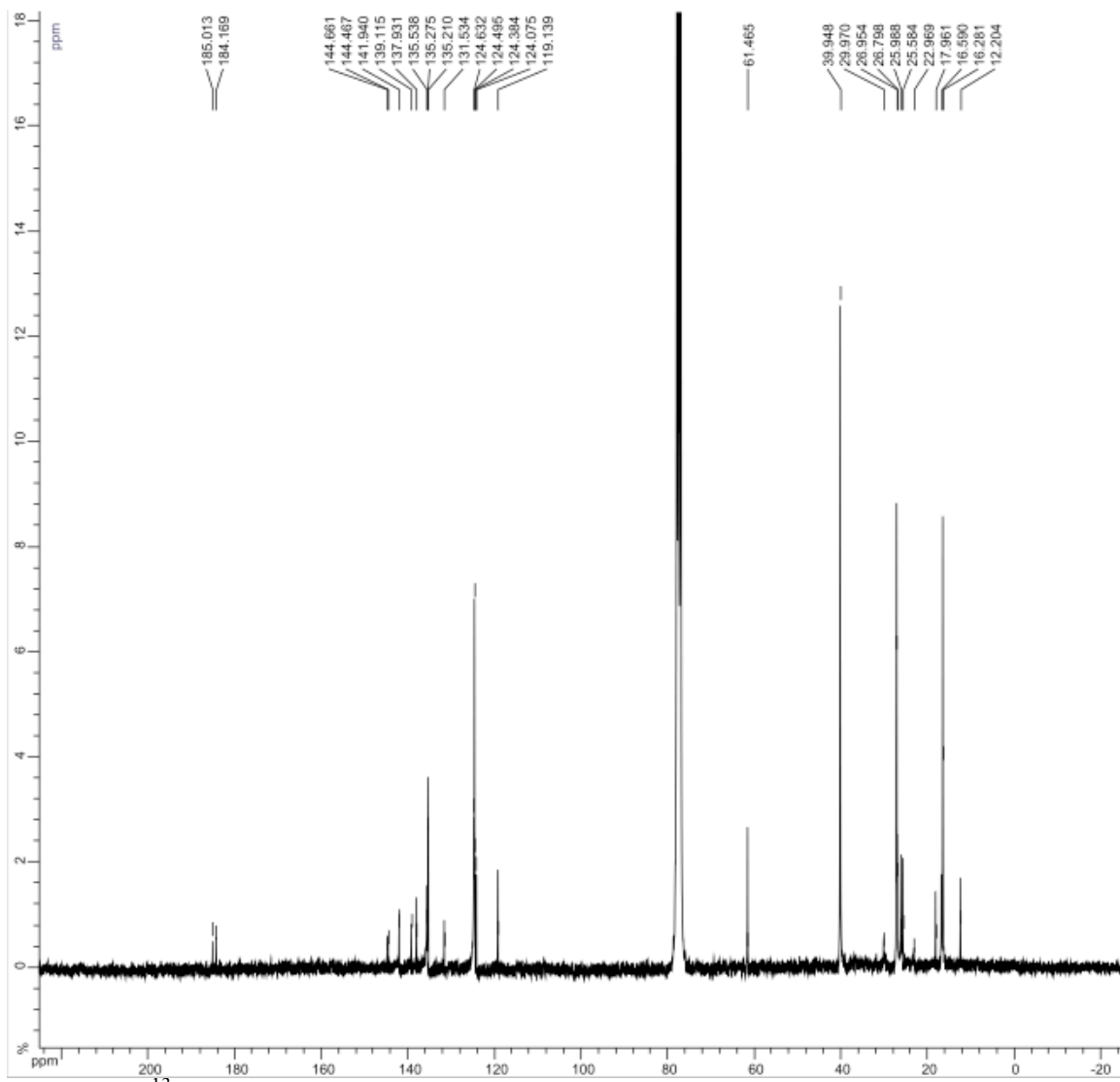


Figure S1. ^{13}C -NMR spectrum of cell membrane extract purified by collecting the HPLC fraction absorbing at 406 nm.

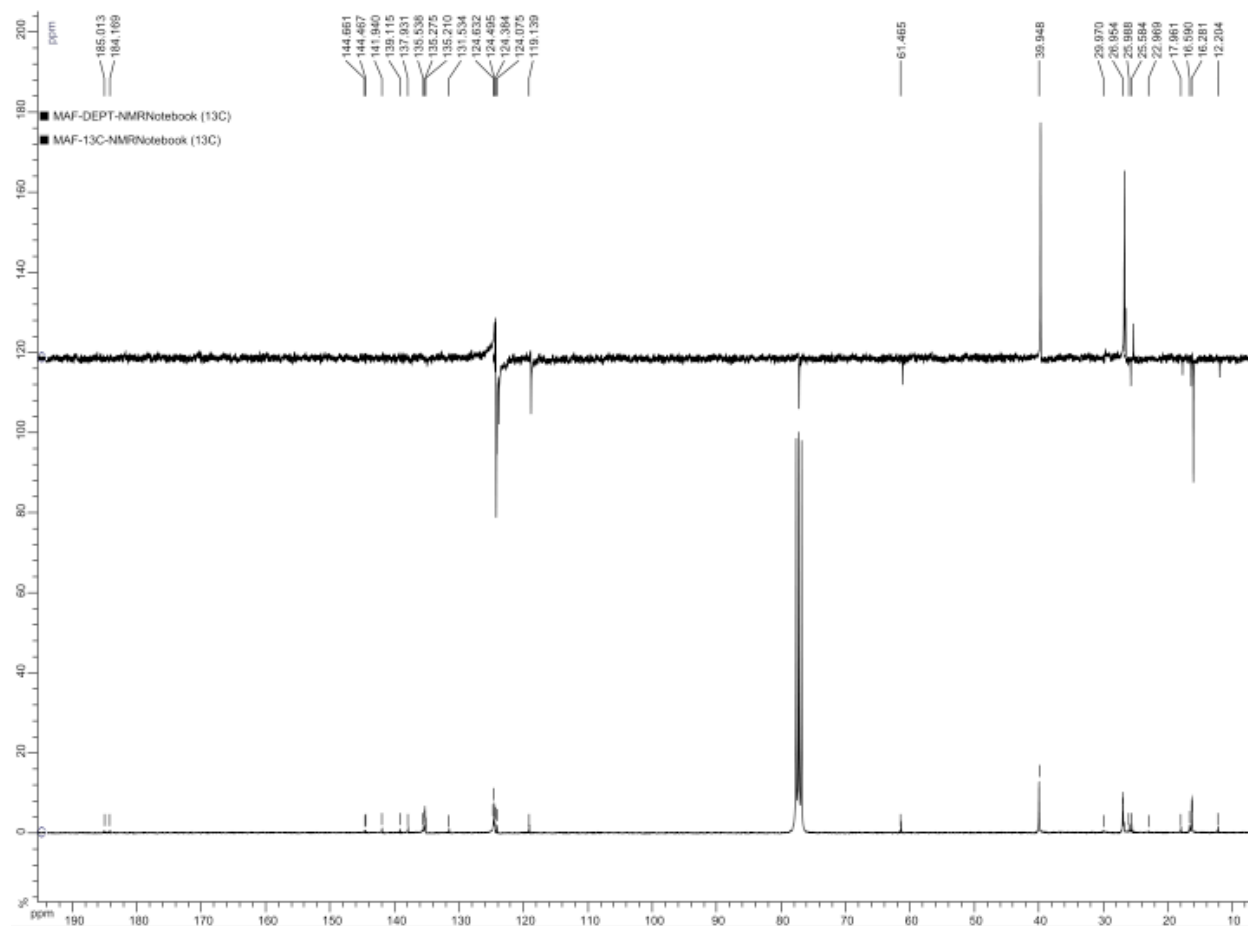


Figure S2. DEPT spectrum coupled with ^{13}C -NMR spectrum for cell membrane extract purified by collecting the HPLC fraction absorbing at 406 nm.

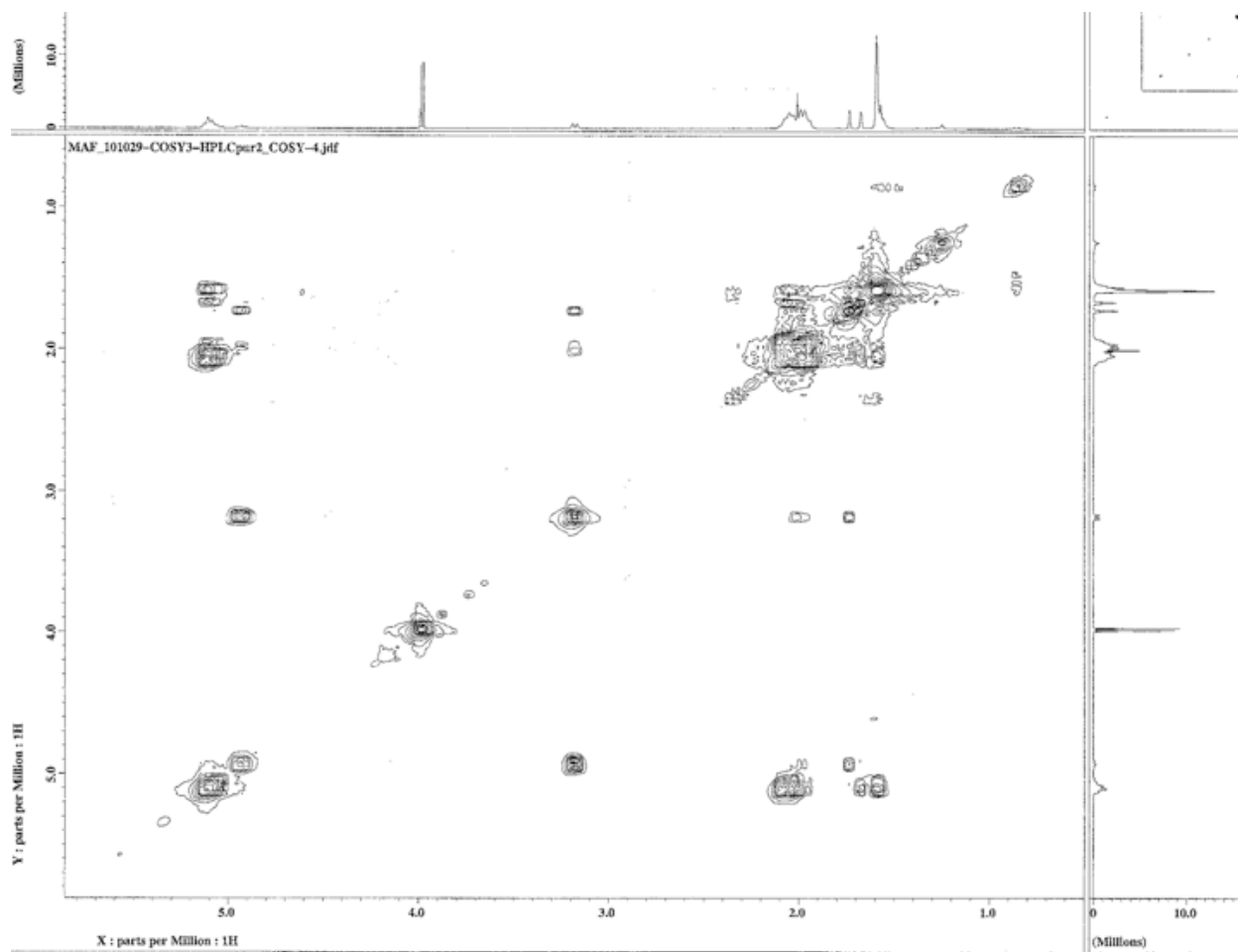


Figure S3. COSY spectrum for cell membrane extract purified by collecting the HPLC fraction absorbing at 406 nm.

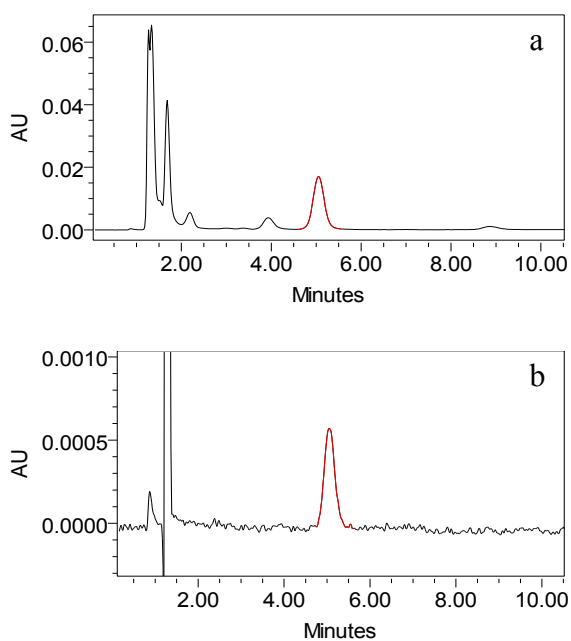


Figure S4: HPLC chromatograms of crude extract (extraction method 2) from dried cells at (a) 275 nm and (b) 406 nm. Quantification was performed at 275 nm due to higher absorbance and better signal to noise ratios, but the chromatogram at 406 nm demonstrates that UQ8 is the compound primarily responsible for the yellow color of cells or cell extract.

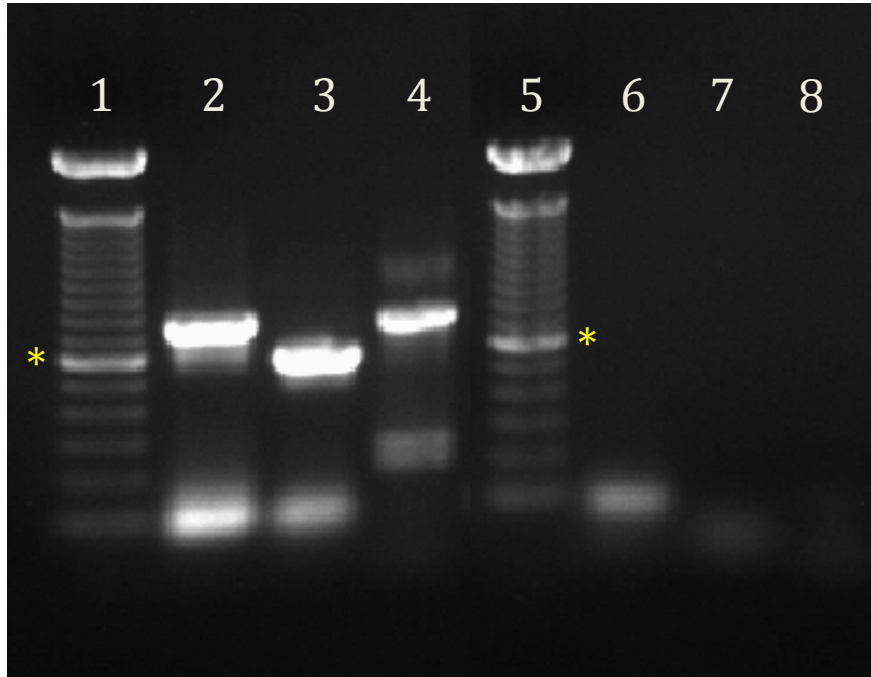


FIGURE S5. Gel electrophoresis of RT-PCR products prepared with *B. bacteriovorus* 109J prey lysate and *E. coli* ML35. Lanes correspond to 100 bp ladders (lanes 1 and 5; asterisk at 600 bp), *B. bacteriovorus* prey lysate with Bd0422, Bd2350, and 16s rRNA primers (lanes 2-4, respectively), and *E. coli* ML35 with Bd0422, Bd2350, and 16s rRNA primers (lanes 6-8). Amplicon sizes for the Bd0422, Bd2350, and 16s rRNA primers are 758, 608, and 765 bp, respectively.

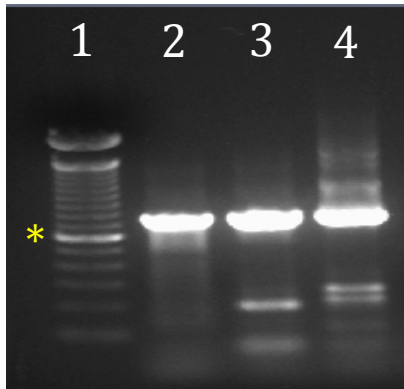


Figure S6. Gel electrophoresis of RT-PCR samples hybridized to 16s rRNA primers. cDNA from the inner region, outer region, and whole film of a spatially organized *B. bacteriovorus* 109J film were used for lanes 2-4, respectively. Lane 1 contains a 100 bp ladder (asterisk at 600 bp). The expected amplicon is 765 bp.

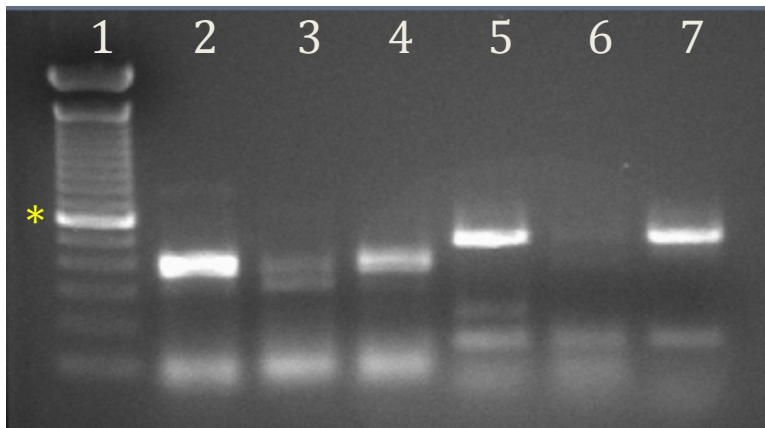


Figure S7. Gel electrophoresis of HindIII digests of RT-PCR samples hybridized to Bd0422 and Bd2350 primers. Lane 1 contains a 100 bp ladder (asterisk at 600 bp). Lanes 2-4 show the Bd0422 primer hybridized to cDNA from the inner region, outer region, and whole film, respectively. Likewise, lanes 5-7 contain the Bd2350 primer hybridized to cDNA from the inner region, outer region, and whole film, respectively. The expected amplicons are 358 and 400 bp for lanes 2-4 and 140 and 468 bp for lanes 5-7.

Table S2. Relative gene expression in HI, 30-min bdelloplasts, and 3-hour bdelloplasts compared to attack-phase bdellovibrios for genes related to flagella or gliding motility. Values in red and blue correspond to up- and downregulated genes, respectively. Dashes indicate no significant change in gene expression. Note that flagella-related genes, are generally down-regulated for both bdelloplasts and HI relative to attack-phase *B. bacteriovorus*, although there is less down-regulation for 3-hour bdelloplasts since the growing *Bdellovibrios* are beginning to develop new flagella by this point. In contrast, gliding motility genes are highly upregulated for HI cells.

Gene Number	Likely gene homolog	X-fold change in HI ^a	X-fold change for 30 min bdelloplast ^a	X-fold change for 3-hr bdelloplast ^b	Gene Number	Likely gene homolog	X-fold change in HI ^a	X-fold change for 30 min bdelloplast ^a	X-fold change for 3-hr bdelloplast ^b
Flagella					Bd3403	fliG	0.40	0.61	0.004
Bd0144	motA	0.35	-	7.25	Bd3404	fliF	0.53	0.68	0.009
Bd0145	motB	-	-	-	Bd3405	fliE	0.17	0.58	0.018
Bd0408	flaA	-	-	-	Bd3406	flgC	0.42	0.42	-
Bd0410	hag	-	0.69	-	Bd3407	flgB	0.58	0.50	-
Bd0530	flgE	0.36	0.54	-	Gliding				
Bd0531	flgG	-	0.56	-	Bd0179	aglW	3.74	-	38
Bd0532	flgA	1.34	0.59	-	Bd0181	aglV	6.29	-	103
Bd0534	flgH	-	-	-	Bd0182	aglX	6.86	-	202
Bd0535	flgI	0.56	0.66	-	Bd0412		2.19	4.54	12
Bd0536	flgJ	-	-	4.69	Bd0413		-	4.58	-
Bd0537	flgM	0.37	0.59	14.03	Bd0414		2.10	5.09	-
Bd0538		0.53	0.52	11.79	Bd0415		4.48	3.93	7
Bd0540	flgK	0.59	0.56	-	Bd0416		1.96	4.45	6
Bd0542	flgL	0.19	-	-	Bd0417		2.05	4.66	9
Bd0604	hag	0.18	-	0.001	Bd0418		3.32	6.89	-
Bd0605		0.36	-	0.016	Bd0419		4.99	5.21	-
Bd0606	hag	0.34	-	0.020	Bd0420	aglR	3.67	7.84	-
Bd0607		1.84	1.71	-	Bd0828		3.59	0.67	11
Bd0608	ppc	0.66	-	-	Bd0829		2.05	-	-
Bd0609		0.07	0.59	0.036	Bd0831		2.79	0.62	-
Bd0610	fliD	0.47	-	-	Bd0832	agmU	1.76	-	-
Bd0611	fliS	0.35	0.61	-	Bd0833	aglT	1.83	-	-
Bd0804	fliL	1.38	-	18.70	Bd0834		6.12	-	-
Bd1076	fliL	0.22	0.69	0.009	Bd0836	aglR	9.63	-	-
Bd2177		0.27	-	-	Bd0837	tolR	8.55	-	-
Bd3014	fliG	-	-	-	Bd0838	aglS	-	-	-
Bd3020	motB	2.20	-	-	Bd1023	gldA	4.63	-	102
Bd3021	motA	0.59	-	-	Bd1024	gldF	21.75	-	63
Bd3052	flgL	0.43	-	0.22	Bd1025	gldG	12.38	-	49
Bd3253	motB	0.40	0.59	0.14	Bd1473		0.63	-	0.021
Bd3254	motA	0.22	0.60	65.50	Bd1474		4.31	-	0.014
Bd3318	fliA	0.43	0.58	0.11	Bd1475		3.76	0.58	0.040
Bd3319	fliN	-	0.67	-	Bd1476		2.03	0.64	0.034
Bd3320	flhF	-	0.56	-	Bd1477		-	0.62	0.035
Bd3321	flhA	-	-	-	Bd1478	agmU	1.33	0.65	0.058
Bd3322	flhB	-	-	-	Bd1479	aglS	2.60	0.67	0.21
Bd3323	fliR	-	0.66	-	Bd1480		3.13	0.57	0.032
Bd3324	fliQ	-	0.50	-	Bd1481	aglR	6.67	0.61	0.11
Bd3325	fliP	0.64	-	-	Bd1482		-	0.69	0.15
Bd3326	fliO	1.34	0.54	-	Bd1483		-	-	0.051
Bd3327	fliN	-	0.56	-	Bd2368		10.55	-	187
Bd3328	fliM	-	0.67	-	Bd2369		10.51	-	86
Bd3329	fliL	0.47	0.60	-	Bd2370		11.49	-	76

Bd3342	hag	0.37	-	-	Bd2371		16.39	-	91
Bd3395	flgE	0.59	0.68	-	Bd2372		5.84	-	64
Bd3397	flgD	0.41	0.49	-	Bd2373		3.10	-	36
Bd3398		1.65	0.53	0.047	Bd2374		7.00	-	120
Bd3399		0.46	0.67	0.063	Bd2375	aglS	7.06	-	155
Bd3400	fliJ	0.64	0.63	0.014	Bd2376		16.51	-	104
Bd3401	fliI	0.55	-	0.009	Bd2377	aglR	33.12	-	694
Bd3402	fliH	0.53	0.60	0.008	Bd3762		3.10	-	33

^a from Lambert *et al.* [14], based on DNA microarrays

^b from Karunker *et al.* [15], based on RNA-seq